

## Tactile Hyperacuity Thresholds Correlate with Finger Maps in Primary Somatosensory Cortex (S1)

Robert O. Duncan<sup>1</sup> and Geoffrey M. Boynton<sup>2</sup><sup>1</sup>Hamilton Glaucoma Center, University of California, San Diego, La Jolla, CA 92093-0946, USA; <sup>2</sup>The Salk Institute for Biological Studies, La Jolla, CA 92037, USA

**Behavioral tactile discrimination thresholds were compared with functional magnetic resonance imaging measurements of cortical finger representations within primary somatosensory cortex (S1) for 10 human subjects to determine whether cortical magnification in S1 could account for the variation in tactile hyperacuity thresholds of the fingers. Across 10 subjects, the increase in tactile thresholds from the index finger to the little finger correlated with the decrease in cortical representation across fingers in S1. Additionally, representations of the fingers within S1, in Brodmann areas 3b and 1, were also correlated with the thresholds. These results suggest that tactile hyperacuity is largely determined by the cortical representation of the fingers in S1.**

**Keywords:** digit, fMRI, hand, skin, somatic, touch

Neuronal response properties in primary sensory areas may depend largely upon the density of connections between thalamus and cortex. For example, angular resolution in primary visual cortex is thought to emerge from the sampling density of cortical neurons representing a particular region of visual space (Stevens 2001, 2002). This prediction is supported by a previous study that reported a correlation between visual acuity at a particular location in visual space and the area within visual cortex representing that location (Duncan and Boynton 2003). In that study, visual acuity at any given location in the visual field was represented by a constant area in the cortex, which implies that the cortical representation of the minimally resolvable spatial distance is represented by a fixed number of neurons in primary visual cortex (V1). Thus, angular resolution may be an emergent property of the sampling resolution (i.e., density) of neurons in V1. Similarly, it is possible that angular resolution in area 2 of human primary somatosensory cortex (S1) may be an emergent property that depends upon the sampling resolution of area 3b. In the present study, we sought to determine whether the relationship between spatial acuity and thalamo-cortical connectivity generalizes to other sensory modalities by comparing behavioral measurements of tactile acuity with the representation of the hand in the human S1.

Understanding the relationship between tactile thresholds and the cortical representation of the fingers is also important because S1 is commonly associated with short- and long-term cortical plasticity. For example, experience and expectations are known to affect tactile performance (Pantev et al. 2001), receptive field sizes of S1 neurons (Xerri et al. 1999), and tactile thresholds (Kennett et al. 2001). Similarly, manipulating attention, sometimes by using multimodal stimulation, is also known to affect somatotopic representations in S1 (Johansen-Berg et al. 2000; Braun et al. 2002; Hamalainen et al. 2002; Meador et al.

2002). Somatotopic representations in S1 have also been shown to be task specific (Braun et al. 2000).

Direct comparisons between behavioral and anatomical data for multiple fingers have not been conducted in the same human subjects. Therefore, this study used functional magnetic resonance imaging (fMRI) to compare the size of individual subjects' cortical finger representations with their behavioral thresholds on a tactile hyperacuity task. Analogous to previous results for visual cortex, changes in tactile hyperacuity thresholds across fingers could be accounted for by differences in the size of the cortical representation for those fingers in S1. Furthermore, variations in the size of the finger representation in Brodmann areas 3b and 1 (within S1) were correlated with variations in hyperacuity thresholds. These results support claims that tactile hyperacuity is ultimately limited by the sampling resolution of S1, particularly Brodmann areas 3b and 1.

### Experimental Procedures

#### Subjects

A total of 10 subjects participated in both the behavioral and fMRI experiments (5 male and 5 female volunteers between 18 and 36 years of age). All participants were right-handed with only 1 subject reporting a childhood history of ambidexterity. One subject was an author (ROD). All analyses were repeated without the data from this author, and no changes to the results or conclusions were made unless noted. Informed consent was obtained in writing, and all studies were conducted with permission from the Salk Institutional Review Board.

#### Behavioral Measurements of Tactile Hyperacuity

Hyperacuity thresholds were measured for the index finger (D2), middle finger (D3), ring finger (D4) and little finger (D5) on each hand using a tactile variation of a visual hyperacuity task devised by Ludvigh (1953) and further developed by Loomis (1979). This task was chosen because it can be thought of as a close tactile analogue to the Vernier acuity stimulus used in a previous study of the visual system (Duncan and Boynton 2003) and is analogous to a visual hyperacuity task, which measures the ability to perform spatial discriminations finer than what is predicted by receptor density (Westheimer 1977; Loomis 1979; Wheat et al. 1995).

Subjects were seated comfortably in a quiet room with their eyes closed. Each subject positioned their arm on a custom-built armrest with their hands and fingers unrestrained. The armrest also hid the stimuli from the subject's view. An Apple G3 PowerBook laptop computer controlled stimulus presentation and data acquisition (PowerBook G3 processor, 300 MHz) using MATLAB 5.2 software with the Psychophysics Toolbox (Brainard 1997; Pelli 1997).

Stimuli consisted of 3 raised bumps that were photoengraved onto a zinc plate (see Fig. 1). The 3 collinear bumps were aligned with the long axis of the finger. The middle bump was slightly offset along the orthogonal axis, and subjects were instructed to report the direction of this offset as "left" or "right" by pressing the numbers "1" or "2" (with their untested hand) on a standard 10-key pad connected to the computer. Bumps were separated along the finger axis by 3 mm, and the

orthogonal offsets ranged from 0.05 to 3.75 mm. Offsets between 0.25 and 3.75 mm changed in step sizes of 0.25 mm, and offsets smaller than 0.25 mm changed in step sizes of 0.05 mm (total set size = 19). The diameter of the bumps was 0.3 mm at the base and 0.05 mm at the tip. The height of the bumps was 0.9 mm. The entire stimulus set was engraved along several concentric circles on the same plate, and the experimenter positioned the appropriate stimulus under the finger of the subject between trials by rotating the plate about its stationary base. Random movements of the disk were introduced during each trial to prevent subjects from using auditory or temporal cues to solve the task. The computer cued the experimenter visually as to which stimulus should be presented.

Hyperacuity thresholds were defined as the just-noticeable difference between the middle bump and the surrounding bumps (in millimeters). Thresholds were obtained twice for each of the 4 fingers on each hand using a staircase procedure (80 trials per staircase) to estimate the offset leading to 80% correct performance. The lateral offset of the middle bump was decreased or increased using a 3-down/1-up procedure (3 correct responses in a row led to a decrease in the offset on the next trial and a single incorrect response led to an increase in the offset). The direction of stimulus offset (left or right) was randomized from trial to trial, and 1 finger from either hand was pseudorandomly selected on each session. Subjects were cued to lightly press their fingers down on the stimulus by a computer-generated tone and were given an unlimited time to respond. To reach threshold in a shorter number of trials, the increment by which offsets were adjusted was larger by one order of magnitude for the first 20 trials. Tactile stimuli were presented to each of 4 fingers and 2 hands randomly, yielding a total of 1280 trials per subject.

For a given session, the data from the staircase were fit with a Weibull function using a maximum likelihood procedure to compute the threshold (80% correct) for that condition. The 3 sessions that did not yield acceptable fits were removed from the analysis and repeated. Thresholds were then averaged across repetitions to obtain a mean threshold for each finger of each subject. Subjects were given a practice session to minimize any potential effects of perceptual learning. These precautionary measures appear to be adequate as there were no systematic changes in performance between the first and the second sessions (analysis of variance [ANOVA],  $P > 0.10$ ).

Subjects complied with the instructions of the task despite the lack of mechanical control of the finger. Mechanical control of the finger was



**Figure 1.** Measuring tactile hyperacuity. Subjects were seated comfortably with their eyes closed. Stimuli consisted of 3 roughly collinear bumps that were photoengraved into a zinc plate. The bumps were aligned with the long axis of the finger. Subjects reported whether the middle bump was shifted to the left or the right of the other 2. The stimulus set consisted of offsets ranging from 0.05 to 3.75 mm, and the entire stimulus set was etched into the same plate. On each trial, the experimenter positioned the stimulus with respect to the subject's finger by rotating the plate relative to its base. The subject pressed down lightly on the stimulus after an auditory cue. Arm motions were prevented with an armrest. Thresholds were determined using a standard 3-up/1-down staircase procedure.

not employed because such devices do not completely prevent undesired movement. Mechanical restriction of the finger also has the added disadvantage of touching the skin with surfaces that are irrelevant to the task. Subjects were instructed not to move their fingers laterally, and were given one opportunity to place their fingers on the stimulus. The experimenter positioned the stimulus and visually inspected the placement of the finger on each trial. On rare occasions when subjects placed their finger incorrectly on the stimulus or moved his/her finger in any direction besides directly up or down, the trial was aborted and the computer randomly chose a new stimulus. Practice sessions were also implemented to ensure subject compliance. Proof of subject compliance is evident in the low variability of the data (Fig. 2), which is consistent with previous studies of tactile spatial resolution (Summers and Lederman 1990; Sathian and Zangaladze 1996; Vega-Bermudez and Johnson 2001). Because of the experience gained from the practice sessions, thresholds are expected to be at a minimum for each observer.

### General fMRI Methodology

The cortical area of each finger representation (cortical magnification) was measured in the same 10 subjects who participated in the psychophysical experiments. The fMR images were acquired at the University of California at San Diego (UCSD).

"Anatomical images" were acquired at Thornton Hospital on the UCSD campus using a 1.5-Tesla Siemens VISION system scanner. These high-resolution ( $1 \times 1 \times 1$  mm) reference volumes of the entire brain were acquired using a  $T_1$ -weighted magnetization prepared rapid gradient echo (MPRAGE) pulse sequence. The controlling computer on the 1.5-Tesla Siemens scanner was equipped with Numaris 3 software using a standard head coil.

"Functional images" were acquired at the Center for Functional Magnetic Resonance Imaging on the UCSD campus using a 3.0-Tesla Varian system scanner. The controlling computer at the Center for Functional Magnetic Resonance Imaging used Varian's resident software package. A small-diameter birdcage head coil was employed (designed by Dr. Eric Wong at UCSD). Subjects lay in a supine position in the bore of the scanner, and their heads were securely positioned with a bite bar. Subjects viewed a projection screen positioned near their neck through an angled mirror. Visual stimuli were back-projected onto the screen using the aforementioned software, laptop computer, and a projector (NEC LT157 LCD video projector, maximum brightness = 1500 lumens, resolution =  $1024 \times 768$ , 60 Hz, equipped with a specialized lens).

During each functional scan, 130 temporal frames were acquired using a low-bandwidth echo planar imaging pulse sequence lasting 260 s (repetition time = 2 s, echo time = 30 ms, flip angle =  $90^\circ$ , 28 axial

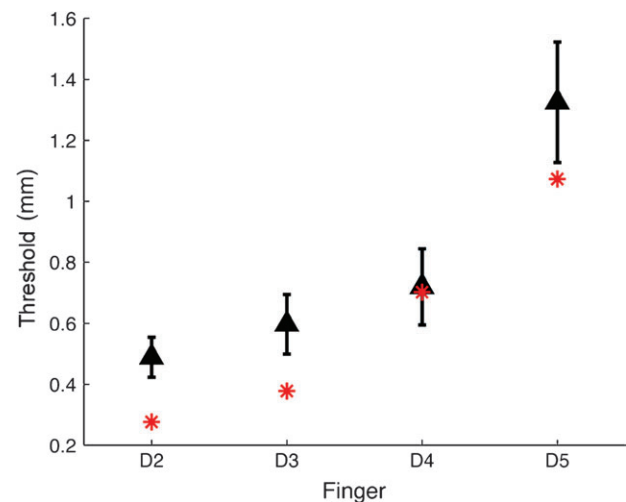


**Figure 2.** Mean hyperacuity thresholds. Hyperacuity thresholds are plotted with respect to each finger. Individual fingers are labeled from the index finger to the little finger as D2–D5. Data points denote the mean thresholds for both hands and all 10 subjects. Error bars indicate the standard error of the mean. Red asterisks represent the predicted psychophysical thresholds derived from our estimates of receptive field size.

slices of 4-mm thickness and  $4 \times 4$ -mm resolution, field of view = 256 mm). The first 10 temporal frames (20 s) were discarded to avoid magnetic saturation effects.

Up to 7 scans were acquired from each subject during each scanning session. These blood oxygenation level-dependent (BOLD) images were used to measure cortical magnification in a succession of scans by locating the regions of cortex that responded to tactile stimulation of each finger. The method of tactile stimulation is described below. Data from each hand were collected in different sessions.

Each scanning session ended with an anatomical scan using a standard  $T_1$ -weighted gradient echo pulse sequence (MPRAGE,  $1 \times 1 \times 1$ -mm resolution). Anatomical scans were used to align functional data across multiple scanning sessions to a subject's reference volume.

Imaging data were transformed from raw Fourier space into image space at the time of scanning using Varian's resident software. The resulting AFNI (available at <http://afni.nimh.nih.gov/>) image data were converted into files that could be read by the analysis suite mrVista (available from <http://white.stanford.edu>). Specifically, AFNI image data corresponding to the high-resolution reference volume and the functional scans were rotated, and image slices were sampled again at  $1 \times 1$ - and  $3 \times 3$ -mm resolutions, respectively. Note that this is a lossless conversion. The reference volume was cropped and used to segment the gray matter from the white matter and the cerebrospinal fluid (CSF). Then, the representation of the gray matter was computationally flattened (described below). The data from the functional scans were processed by 1) dividing each voxel's time series by its mean intensity, and 2) subtracting any linear trend from each voxel's time series. Each in-plane image was individually corrected for head motion using rigid-body motion compensation. In-plane images were aligned to a reference scan using affine transformation.

### **fMRI Somatotopic Stimulation Paradigm**

Measurements of the hand representation in S1 have been complicated by the significant amount of overlap between adjoining regions of fMRI activity. There is evidence suggesting that this overlap is biological in origin (Shoham and Grinvald 2001). Nonetheless, the spatial blurring of the hemodynamic response, a problem inherent to fMRI, accounts for much of the overlap. For these reasons, a strategy originally employed to measure the representation of the fingers in primary motor cortex was adopted (Dechent and Frahm 2003). Unlike traditional block designs that stimulate each finger in alternation with a resting period, each finger was stimulated in alternation with another finger on the same hand (e.g., 20 s stimulating D2 vs. 20 s stimulating D4).

Each pair of fingers was stimulated in alternation for six and a half 40-s cycles (data from the first half cycle were discarded to avoid magnetic saturation effects). All possible finger combinations were conducted, yielding a total of 6 scans for each hand. Finally, the 3 scans corresponding to a given finger (e.g., D2 vs. D3, D2 vs. D4, and D2 vs. D5) were then averaged. This technique results in a robust somatotopic map for each finger (in this case, D2) with little or no overlap between adjoining finger representations.

Somatic stimulation was carried out using a plastic painter's brush covered in soft sponge. Tactile stimulation was performed in synchrony with a flashing visual stimulus ( $3 \times 3$  degrees, 4-Hz flicker, 100% contrast). The finger to be stimulated was cued visually by alternating the shape of the visual cue from a circle to a square every 20 s. Subjects gripped a plastic tool with the index, thumb, and middle finger of the nonstimulated hand (much like one would hold a pencil) and moved the fingers of the nonstimulated hand. The stimulated hand rested on the subject's thigh in a fixed position on its side, and both hands were kept still (except for the finger motion of the stimulating hand). The fingers of the stimulating hand were allowed to move, but the wrist and the palm remained still. Subject compliance was determined by a post-scanning interview, by monitoring a practice session outside of the scanner, and by visually inspecting the stimulation during each scan. Subjects stroked the full length of the glabrous skin on the stimulated finger from tip to base with a medium-intensity stroke (strong enough to avoid the sensation of tickling but weak enough to avoid pain or irritation). The frequency of the stroke was 4 Hz. The mean speed of the stroke was  $6.9 \text{ mm/s}^2$  ( $\pm 0.83$  standard deviations based on the variation in finger length between subjects) and the range was 5.1–8.6  $\text{mm/s}^2$ .

Subjects were instructed to maintain a consistent quality of motion throughout the duration of the scan. To minimize motion artifacts, subjects were instructed to move the plastic tool by using their fingers and keeping the wrist as still as possible.

Although this method of self-stimulation is not optimally controlled, robust patterns of activity in the hemisphere contralateral to the stimulated fingers were observed, and there was no systematic pattern of activity in the hemisphere contralateral to the stimulating hand. The order of finger stimulation both within and across subjects was counterbalanced so that the first scanning session in half the subjects began with stimulation of the right hand. Also, the order of the finger pairs that were stimulated was selected in a pseudorandom order within each scanning session. The experimenter told the subject which finger pair should be stimulated during each scan, and the subject repeated the instructions back to the experimenter via an intercom. Postscanner interviews and observations indicated that subjects could easily stimulate the appropriate regions of the finger, even without visual feedback.

Previous studies have demonstrated effects of training and experience on the representation of fingers in human S1 (Pascual-Leone and Torres 1993; Elbert et al 1995; Braun et al. 2000; Candia et al. 2003). To avoid these potential short-term changes in the hand representation caused by training, fMRI imaging was conducted before the behavioral sessions, and measurements for each finger were interleaved in all functional and behavioral sessions.

Another set of studies suggests that S1 maps change with the focus of attention (Buchner et al. 1999; Noppeney et al. 1999; Braun et al. 2000; Buchner et al. 2000; Ziemus et al. 2000; Braun et al. 2002). Performance on our task was not quantitatively monitored. However, this task was sufficiently engaging, keeping the subject focused on the finger of stimulation for the duration of the scan. Most importantly, as described below, estimates of cortical magnification depend on the location of the peak fMRI response and not the magnitude. Hence, modulating factors such as stimulation strength and attention should not have an influence on the results.

### **Estimating the Borders of S1 Using Anatomical and Functional Criteria**

The borders of primary somatosensory cortex were initially estimated using anatomical landmarks. Activity maps were projected onto flattened representations of the cortex, which were derived using standard procedures for segmentation and cortical flattening (Engel et al. 1994; Sereno et al. 1995; Boynton et al. 1999; Duncan and Boynton 2003). During segmentation, gray matter was identified in the high-resolution reference volume using a Bayesian classification algorithm (Teo et al. 1997). Mean image luminance values corresponding to the gray, white, and CSF voxels were first computed by sampling contiguous regions ( $\sim 5 \times 5$  mm) in the in-plane images. The software automatically constructed a volume corresponding to the white matter. The volume of white matter was checked by the user for "cavities," non-white matter regions that were surrounded by white matter, and "handles," regions where the volume connects to itself like the handle of a coffee cup. After these artifacts were corrected by altering pixels in the white matter volume, gray matter was grown from the contiguous volume of white matter in a series of 1-mm layers (less than 6) that originated at the white matter boundary. Gray matter growth was limited by 1) the thickness of the gray matter, 2) the presence of CSF, and 3) collisions with gray matter originating from neighboring regions.

Cortical distances were determined using flat maps that were obtained for each hemisphere and for each subject. Cortical flattening procedures are described in detail elsewhere (Engel et al. 1997). First, an automated algorithm assigned sample positions to the three-dimensional (3D) cortical manifold. Then, these points were projected onto a planar surface and adjusted using an iterative multidimensional scaling algorithm. Finally, the positions of the remaining gray matter points on the flattened surface were interpolated.

A multidimensional scaling algorithm was used to computationally flatten the postcentral gyrus for each hemisphere (Engel et al. 1997). Multidimensional scaling is useful because it enables visualization of the distances between finger representations in a standard frame of reference, specifically, perpendicular to the long axis of the finger on the flattened cortical representation. By reducing the degrees of freedom

to one dimension, analyzing cortical distances on the flattened representation eliminates the influence of extraneous variance that is unrelated to the issue of cortical magnification. Approaches that measure the Euclidean distance in the 3D reference volume often do not take cortical curvature into account and may underestimate the distance between finger representations. After the functional data were projected onto the flattened representation, the boundaries of somatosensory areas were delineated by hand. Finally, after the borders of S1 were estimated, a smaller area of the cortex around S1 was reflattened to minimize any distortions created by flattening.

To create parameter maps of fMRI responses to finger stimulation, the time course of the fMRI response from each voxel was cross-correlated with a sinusoid corresponding to the expected stimulus frequency (40-s period), using a delay in phase associated with the typical hemodynamic response (Boynton et al. 1996). The resulting amplitude maps topographically illustrate the sign and strength of the correlation between the BOLD signal and the stimulation of each finger.

A combination of functional and anatomical criteria was used to identify S1 (specific anatomical criteria discussed in the next section). Because sulci and gyri were visible on the flattened representation of the cortex, it was easy to locate the postcentral gyrus and flatten a small region of cortex corresponding to this region to minimize distortions. The activity patterns were also checked to confirm that the medial/lateral order of the finger representations was in agreement with the anatomical literature, and that the long axis of the finger representations was properly oriented along the anterior/posterior axis.

#### ***Estimating the Borders of Brodmann Areas within S1 Anatomically***

Area S1 is divided cytoarchitecturally into 4 distinct regions: Brodmann areas 3a, 3b, 1, and 2 (Brodmann 1909; Vogt C and Vogt O 1919). The contralateral surface of the body is represented within each area (Merzenich et al. 1978; Kaas et al. 1979; Nelson et al. 1980; Sur et al. 1980; Kaas 1983; Pons et al. 1985), and each area demonstrates sensitivity to different qualities of tactile stimulation. Neurons in areas 3a and 2 respond to stimulation of deep mechanoreceptors, whereas neurons in areas 3b and 1 respond to stimulation of superficial mechanoreceptors (Powell and Mountcastle 1959; Iwamura et al. 1993). Accordingly, it was necessary to anatomically segment each area from its neighbor to obtain independent measurements of cortical magnification for each area within S1. It was predicted that cortical magnification in areas 3b and 1 would correlate with the hyperacuity thresholds. By contrast, areas 3a and 2 were not expected to correlate with the hyperacuity thresholds because the stimulus presumably drives the neurons in these areas less effectively.

The techniques adopted to estimate the regions within S1 using anatomical landmarks have been successfully applied many times before (Allison et al. 1989; Gelnar et al. 1998; Francis et al. 2000; Moore et al. 2000; Blankenburg et al. 2003; Overduin and Servos 2004). For each area within S1, the macroanatomical and cytoarchitectonic borders are correlated (Ono et al. 1990; Rademacher et al. 2001) and can be identified using the patterns of sulci and gyri visible in MRI (Sobel et al. 1993). Although there is intersubject variability, macroanatomical and cytoarchitectonic estimations of areas within S1 are in agreement (Zilles et al. 1995; Geyer et al. 1997; White et al. 1997; Geyer et al. 1999; Rademacher et al. 2001). The sigmoidal shape of S1 is visible from the coronal images (Rumeau et al. 1994). The hand area of S1 was estimated by first finding the hand area of primary motor cortex (M1) using anatomical landmarks and then looking at the sulci and gyri posterior to M1 to find the hand region of S1. The omega- or epsilon-like shape of M1 in the axial images is easily identified (Yousry et al. 1997), and this method has been verified as a reliable means of localization (Towle et al. 2003).

Once the hand region was localized, the patterns of sulci and gyri in the 3D high-resolution anatomical MR images and in the flattened cortex were inspected to estimate the location of areas 3a, 3b, 1, and 2 in each subject. A control region of interest (ROI) was also defined for the estimated borders of area 4, primary motor cortex, which lies anterior to area 3a. Sulci and gyri were rendered on the flattened representation as dark and light bands, respectively. The ROIs for areas within S1 were created by manually tracing the pattern of sulci and gyri indicated by the image intensity in the flat map. The ROIs were independently determined for each individual and each hemisphere, and the cortical

distances were measured along the flattened hemisphere of each individual independently.

BOLD data were transferred to the flattened cortical surface according to a procedure described by Engel et al. (1997). First, corresponding anatomical landmarks on the functional in-plane images and the 3D reference volume were determined by the user. Then, the 2 images were aligned using an iterative (least squares) translation (Arun et al. 1987). Each gray matter location on the flattened representation that fell within the functional in-plane images was assigned a functional value. The regions on the flattened surface that did not receive a functional value from the in-plane images were assigned one via interpolation. Each interpolated pixel assignment was the weighted average of the neighboring voxels (i.e., the Gaussian function of the distance to the nearest neighboring pixel).

The borders of area 3a were estimated as the fundus of the central sulcus, area 3b as the posterior wall of the central sulcus, area 1 as the crown of the postcentral gyrus, area 2 as the anterior wall of the postcentral sulcus, and area 4 as the region spanning the posterior wall and the crown of the precentral gyrus. ROIs for each area within S1 were defined on the flattened representation and projected back to the 3D reference volume for visual inspection using the mrVista toolbox for MATLAB (available from <http://white.stanford.edu>).

Once each area within S1 was estimated using anatomical landmarks, templates were fit to the functional data projected on flattened representation of cortex and computed cortical magnification as described below. However, for voxels residing outside of the ROI, the amplitude of the BOLD response was set to zero. Consequently, only voxels within the ROI could influence the fitting of the template to the BOLD data, resulting in independent measurements of cortical magnification for each area within S1. To prevent the template from rotating 90° in parallel with the long axis of the brain areas, a parameter to fit the rotation of the template was not included. Instead, the rotation parameter from the best fitting template from the S1 fits was included.

## **Results**

### ***Hyperacuity Thresholds***

Psychophysical thresholds, averaged across both hands of all 10 subjects, are plotted for each finger in Figure 2 (black triangles). The asterisk symbols are a prediction of the results and are described in a later section. Each data point represents the mean of 20 measurements. Error bars represent the standard error of the mean. Mean thresholds increase monotonically from the index finger to the little finger, and the little finger was significantly different from the other fingers (Scheffé test, all  $P < 0.008$ ).

Even though there was a trend for the nondominant hand to be more sensitive, this trend was only borderline significant (ANOVA,  $P = 0.0513$ ). Without the data from the author ROD, this result was significant ( $P < 0.05$ ). Despite the similarity to previous reports (Meador et al. 1998), claims regarding handedness are cautiously avoided because previous positive results were shown to be task specific (Summers and Lederman 1990), and the generalization of this phenomenon was not tested using multiple stimuli. Furthermore, a more complete study with left-handed participants must be conducted before conclusions regarding handedness are made. No effect of gender on tactile hyperacuity was observed (ANOVA, all  $P > 0.10$ ). Contrary to previous observations of a correlation between age and hyperacuity (Stevens and Patterson 1995), no such correlation was found in this study (all  $P > 0.10$ ), which was probably due to the narrow age range of the subject population.

### ***Measurements of Cortical Magnification***

Figure 3F displays an individual subject's results projected onto a 3D reconstruction of the anatomical reference volume. Each color indicates fMRI responses to stimulation of a different

finger. Regions within S1 were projected onto the reference volume if they possessed a correlation value greater than 0.27. Voxels that showed responses to more than 1 finger were given the color that represents the finger producing the greater response (the analysis for Figure 3F is for illustration purposes only and is separate from methods for measuring cortical magnification).

The gray-scale images in Figure 3A–D show the pattern of responses elicited by stimulating each finger on the flattened representation of S1 in the left hemisphere of an example subject. Bright regions correspond to locations where changes in BOLD signal correlate positively in time with the stimulation of the finger of interest. Stimulation of each finger results in a unique pattern of activity. The characteristic bands of activity are arranged rostral-caudally, with responses to the index finger located lateral to those of the little finger (Fig. 3A–D). Dark regions correspond to negative BOLD signal, which indicates possible neural suppression (Smith et al. 2004). These dark regions vary between fingers because, in the averaging paradigm, the middle (D3) and ring (D4) fingers are compared with fingers that lie to either side, whereas the index (D2) and little fingers (D5) are compared with fingers that lie only to one side. It should be noted that a negative BOLD signal was also evident in the previous study of visual acuity where no differential averaging was done (Duncan and Boynton 2003).

To parameterize the overall somatotopic map of the fingers in S1, the patterns of fMRI responses on the flattened representation of cortex were fit using a template composed of 4 parallel line segments, 1 for each stimulated finger. Seven parameters describe the line segments of the template; their length ( $k$ ), position ( $d_x$ ,  $d_y$ ), rotation ( $d_a$ ), and the distance between each finger ( $a_1$ ,  $a_2$ ,  $a_3$ ). Fits to the maps of each finger were obtained

by adjusting template parameters to maximize the image intensity (i.e., the line integral) under each line segment. Optimized fits to the data from each finger for the hand of a single subject are illustrated as differently colored lines and are superimposed upon the gray-scale correlation maps in Figure 3A–D.

Best fitting parameter values were obtained by an unconstrained nonlinear optimization routine in MATLAB using the following steps. First, a generic template was generated using parameter values ( $a_1$ ,  $a_2$ ,  $a_3$ , and  $k$ ) that roughly corresponded to the size of S1. The center of activity for fMRI responses to the index finger and the little finger were then computed. Next, the origin of the template was moved to the locus of the index finger representation, and the template was rotated about its origin to match the angle of the line segment connecting the little finger and the index finger representations. Lastly, the templates were fit to the correlation maps using a 2-stage optimization routine. In the first stage, each individual model parameter was optimized to fit the template to the maps of all 4 fingers simultaneously. In the second stage, the best fitting template was generated by simultaneously fitting all parameters to the maps. The parameter for finger length,  $k$ , was excluded from the final optimization because, without an objective constraint on finger length, the fit would converge to the trivial condition of a single point over a location of maximum amplitude.

The final best fitting template for the representative subject in Figure 3 is superimposed upon the parameter map for the index finger and presented in panel 3E. The distance along the cortex between the index and middle fingers is clearly larger compared with the distance between the ring and little fingers.

Some of the banding in Figure 3F is due to spatial blurring of the fMRI response and some is presumed to be biological in origin (Shoham and Grinvald 2001). The individual fits in

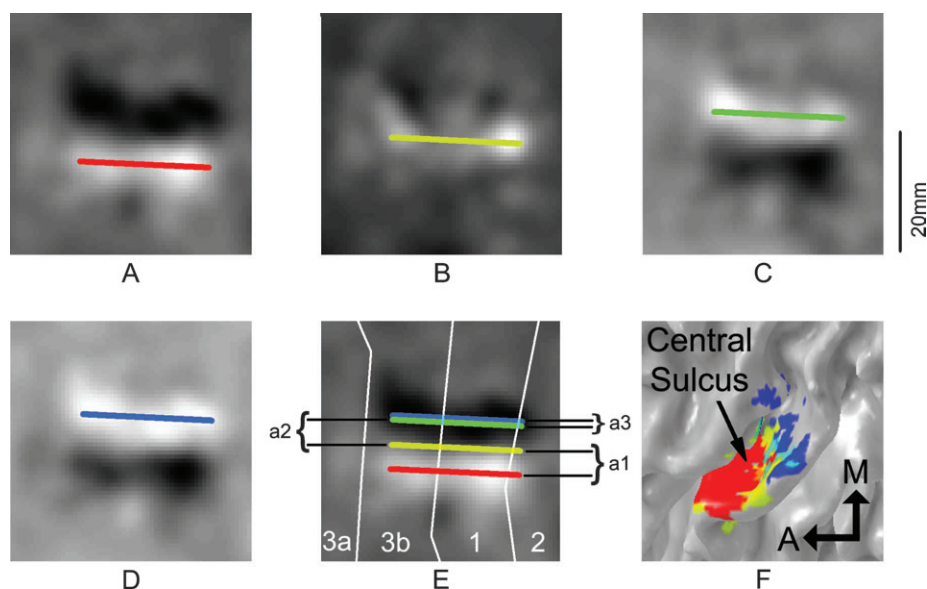


**Figure 3.** fMRI responses to finger stimulation for a single subject. Gray-scale images illustrate the fMRI responses to finger stimulation for the left hemisphere of a single subject (ROD). The computational flattening of each image is identical. Bright pixels correspond to increased BOLD signal that correlates with stimulation of the finger. Each panel represents the mean of 3 scans. In each scan, fMRI responses to stimulation of a particular finger are compared with responses for the other 3 fingers. Superimposed colored lines represent the components of the best fitting template to the data. (A–D) Responses to stimulation of the index, middle, ring, and little finger, respectively. (E) The best fitting template to the data is presented atop the responses for the index finger. Template parameters  $a_1$ ,  $a_2$ , and  $a_3$  that correspond to distances between finger representations are indicated with brackets. A calibration bar is presented at upper right. (F) The functional data are projected onto a 3D representation of the anatomical data. Data in this panel have correlation thresholds of 0.27, and the color-coding scheme is analogous to that for panel E. White lines indicate the borders between areas within S1 (3a, 3b, 1, and 2) and primary motor cortex (area 4), which were determined using anatomical features in the reference volume and flattened cortical surface.

Figure 3A-D illustrate that the spatial blurring of the BOLD response is similar for all finger representations. Similar to the results of Shoham and Grinvald (2001), Figure 3F illustrates that the overlap is larger for the ring finger and little finger compared with the index finger and middle finger. Thus, the banding in Figure 3F does not obscure any detail that is not made evident in Figure 3A-D. On the contrary, this banding actually illustrates the differences in cortical magnification across finger representations.

Figure 4 shows the best fitting templates for each of the 10 subjects for each hemisphere. The subject from Figure 3 is

replotted in the upper-left panel of Figure 4. White lines indicate the estimated borders of areas 4, 3a, 3b, 1, and 2 from left to right (area 4 is not pictured for the left hemisphere of the first subject because it was out of frame). Images from the right hemisphere are flipped to match the orientation of those from the left hemisphere. The overall size of S1 (measured as the distance between the little and index finger representations) varied greatly between hemispheres and subjects. For example, for the subject with the largest hemisphere asymmetry, the smaller representation was 40% the size of the larger (8 vs. 21 mm). The range across all subjects was 8-23 mm, with the smallest

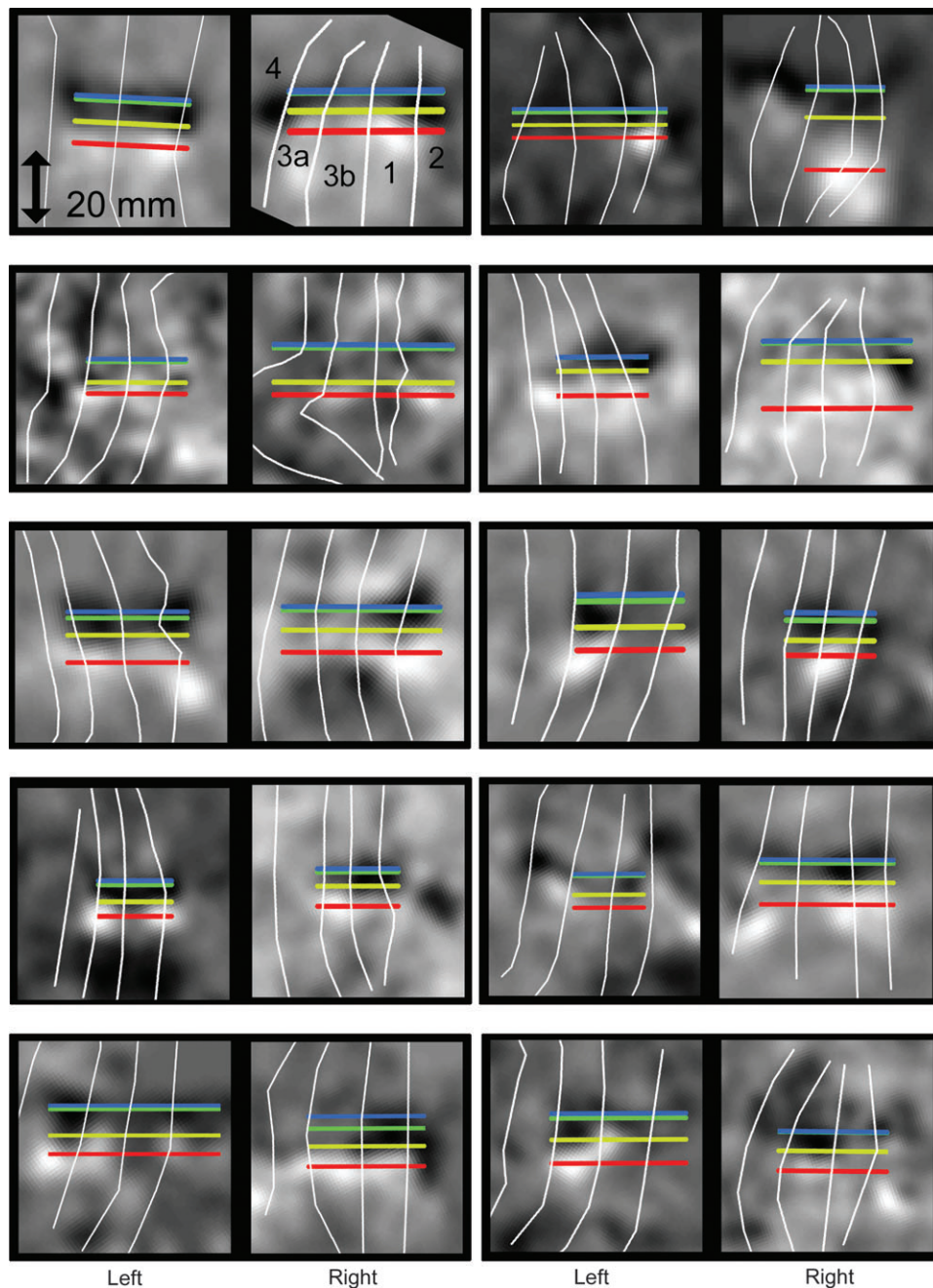


**Figure 4.** Best fitting templates for S1 of all 10 subjects. Each panel contains a best fitting template to the finger representations in each hemisphere of each subject. Red, light green, dark green, and blue lines correspond to fingers D2-D5, respectively. In each panel, templates on the left correspond to the left hemisphere. White lines indicate the estimated borders of areas 4, 3a, 3b, 1, and 2 from left to right. Images from the right hemisphere are flipped to match the orientation of those from the left hemisphere. The fMRI responses from the subject in Figure 3 appear here at top left.

representation being 36% of the largest. This nearly 3-fold variation between individuals is similar in magnitude to previous results reported in owl and squirrel monkeys (Merzenich et al. 1987) and is also similar to the variation observed in the human primary visual cortex (Duncan and Boynton 2003). The mean distance between the index finger and the little finger in this study was 13 mm. As for the example subject in Figure 3, the cortical distance between responses to the index (D2) and the middle finger (D3) tends to be larger than the distance between the ring finger (D4) and the little finger (D5). The mean distances between D2–D3, D3–D4, and D4–D5 were  $6.2 \pm 1.3$ ,  $5.7 \pm 0.6$ , and  $1.1 \pm 0.3$  mm, respectively (95% confidence intervals).

Traditional approaches to measuring cortical magnification compute the width of the band of significant fMRI activity elicited by stimulating each finger on a statistical parameter map (i.e., the width of the bright bands in Fig. 3A–D). However, this method greatly overestimates cortical magnification because the hemodynamic blurring inherent in fMRI inflates estimates based on this measurement. Estimates from this method are highly dependent upon the choice of threshold used for the statistical parameter maps and are also affected by the strength and signal-to-noise ratio of the BOLD signal.

Therefore, cortical magnification was estimated from parameters describing the 3 distances between peak responses associated with the 4 fingers ( $a1$ ,  $a2$ , and  $a3$ ). Mean distance in cortex is plotted for each pair of fingers in Figure 5. The cortical distance between the ring and little finger ( $a3$ ) was significantly smaller than distances between the other fingers ( $a1$  or  $a2$ ) (Scheffé test, all  $P < 0.0167$ ). This agrees qualitatively with the decrease in tactile hyperacuity from the index finger to the little finger (Fig. 2). Neither was an overall effect of laterality between the hemispheres found (ANOVA,  $P > 0.10$ ) nor was there a significant interaction (ANOVA,  $P > 0.10$ ). Furthermore, there

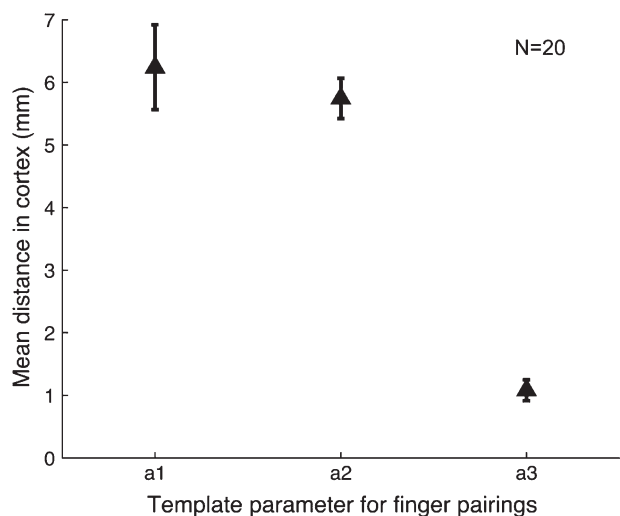


**Figure 5.** Cortical distance as a function of finger pairing. Each template was used to compute an individual estimate of cortical magnification for each hemisphere. Linear cortical magnification was derived from the distance between fits to individual finger representations, which correspond to template parameters  $a1$ ,  $a2$ , and  $a3$ . The template parameters estimate the distance between the cortical representation for fingers D2–D3, D3–D4, and D4–D5, respectively. Data points represent the cortical distance averaged across 20 hemispheres for each template parameter. Error bars represent the standard error of the mean.

was no significant main effect or interaction for a comparison of gender and cortical magnification (ANOVA, all  $P > 0.10$ ). A correlation between cortical magnification and the age of the participants was also not observed ( $P > 0.10$ ).

### Comparing Hyperacuity Thresholds with Cortical Magnification

The 4 hyperacuity thresholds (one for each finger) cannot be directly compared with the 3 template parameters that estimate cortical magnification ( $a1$ ,  $a2$ , and  $a3$ ). Therefore, both data sets were fit with power functions, and the power functions' parameter values were compared. The behavioral thresholds for each hand were fit with the function:  $T = \beta d^p$ , where  $d$  is the finger number (D2, D3, D4, or D5), and  $T$  is the hyperacuity threshold.  $\beta$  describes overall sensitivity across all fingers, and  $p$  provides a measure of the change in psychophysical thresholds across fingers.

Similarly, the fMRI data were fit with a power function,  $M = \gamma a^q$ , where  $a$  is the template parameter ( $a1$ ,  $a2$ , or  $a3$ ) and  $M$  is cortical distance. The  $\gamma$  parameter describes the overall cortical distance across fingers D2–D5, and  $q$  provides a measure of the change in cortical magnification across fingers. A log transform was applied to the  $p$  and  $q$  parameters before using linear statistics to compare psychophysical and fMRI data. The log transformations were required to reduce variability that would have been introduced by fitting nonlinear data sets with linear functions.

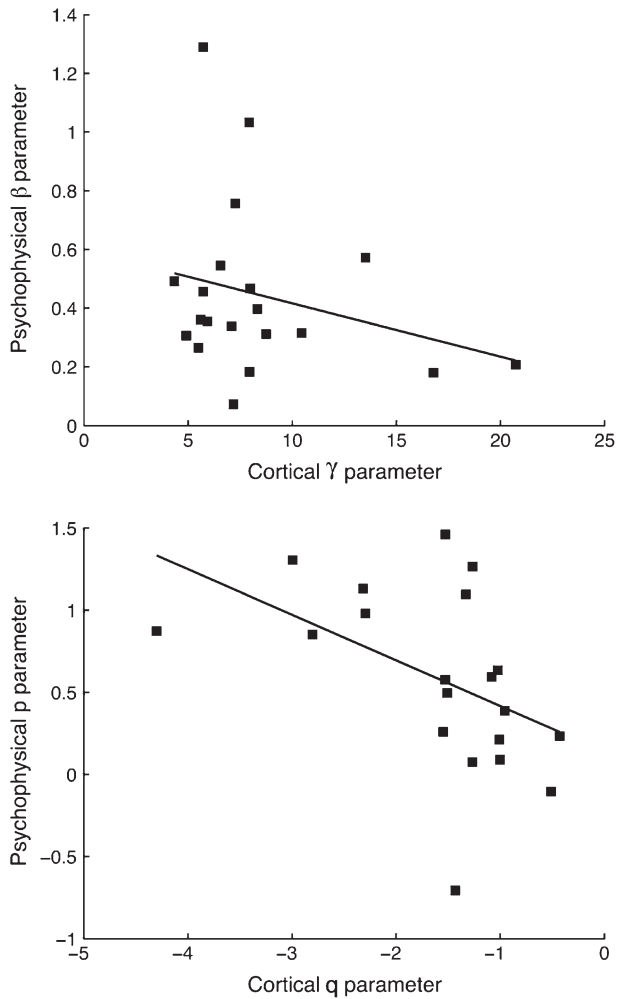
If overall hyperacuity is related to the size of the representation for all 4 fingers within S1, then subjects with smaller overall hyperacuity thresholds should have a larger amount of cortex representing the 4 fingers (i.e.,  $\gamma \approx 1/\beta$ ).

Figure 6A plots  $\gamma$  versus  $\beta$  for each hand in each of the 10 subjects (20 data points in total).  $\gamma$  and  $\beta$  are inversely related, with a correlation coefficient of  $-0.26$ ; however, this negative correlation was not significant ( $P > 0.10$ ) based on a Monte Carlo simulation (see below). Tactile thresholds across all 4 fingers could not be predicted from the overall size of the representation of the 4 fingers in S1.

If, after accounting for overall sensitivity and cortical area of S1, thresholds for a given finger are related to the size of the representation for that finger within S1, then fingers with small psychophysical thresholds will be represented by larger amounts of cortex (i.e.,  $p \approx 1/q$ ). This relationship implies that subjects with a large increase in tactile thresholds from the index to the little finger would have a corresponding decrease in the cortical representations of those fingers.

In Figure 6B, the negative correlation between the  $p$  and  $q$  parameters ( $r = -0.47$ ) was significant both with ( $P < 0.05$ ) and without ( $P < 0.05$ ) outliers based on the Monte Carlo analysis. Note that the correlation describes the “change” in cortical magnification with the “change” in hyperacuity thresholds. These Monte Carlo simulations conclusively demonstrate that there are real within-subject correlations between hyperacuity thresholds and cortical magnification.

The significance of the correlation values was estimated using a Monte Carlo simulation as follows. Each of the 20 curves capturing the change in thresholds across fingers (10 subjects  $\times$  2 hands) was randomly associated with 1 of the 20 curves representing the change in cortical magnification. For each population of random pairings, the correlation coefficients between  $\beta$  and  $\gamma$  and between  $p$  and  $q$  were computed. Our



**Figure 6.** Comparison between cortical magnification and psychophysical thresholds. A comparison was made between cortical magnification and hyperacuity thresholds for each hemisphere/hand of each subject. Changes in cortical distance associated with template parameters  $a1$ ,  $a2$ , and  $a3$  were fit with the power function  $M = \gamma a^q$ . Changes in hyperacuity across fingers were fit with the power function  $T = \beta^p$ . Correlations were determined by comparing parameters for psychophysical and physiological data sets. (A) The correlation between the  $\beta$  and  $\gamma$  parameters for cortical magnification and the psychophysical data sets. Each data point represents the data for a single hemisphere/hand of each subject. (B) The correlation between the  $p$  and  $q$  parameters for cortical magnification and the psychophysical data sets. A Monte Carlo simulation revealed that the probability this correlation could occur was significant below chance.

observed correlations were compared with the population of correlations associated with random pairings to obtain a test statistic.

A secondary analysis was also performed to confirm the validity of the curve-fitting approach. When the psychophysical thresholds from neighboring fingers are averaged, the resulting 3 means can be directly compared with the 3 cortical distances ( $a1$ ,  $a2$ , and  $a3$ ) for each subject. Using this approach, a correlation between the thresholds and cortical magnification was observed ( $r = -0.39$ ,  $P = 0.0023$ ,  $n = 60$ ). Furthermore, a correlation ( $r = -0.50$ ,  $P = 0.028$ ) between  $a3$  and the mean thresholds for D4 and D5 was observed when 1 outlier was removed due to heterogeneity ( $r = -0.42$ ,  $P = 0.06$ , with the outlier). Thus, most of the variance in the correlation appears to be attributable to D4 and D5. The primary results,

analyses, and conclusions are supported by this secondary analysis.

### ***The Relationship between Hyperacuity and Cortical Magnification for Areas within S1***

Similar to the main results, significant correlations between hyperacuity thresholds and cortical magnification were found for several brain areas within S1 (Fig. 7). Anatomical methods were used to define ROIs for areas 1, 2, 3a, 3b, and 4. Subsequent fitting of templates to the BOLD responses in these areas was constrained by the ROI. The method of curve fitting resulted in a set of  $\beta$ ,  $\gamma$ ,  $p$ , and  $q$  parameters for each area. Due to the decreased cortical area of these S1 subregions, the iterative fitting procedure was occasionally unable to yield a reliable template (roughly 1 in 10 fits). Nevertheless, the unreliable fits were easily identifiable as statistical outliers in the distribution of all parameters, and these outliers were removed from the final analysis. Using a Monte Carlo simulation, the psychophysical  $\beta$  and  $p$  parameters were significantly correlated with the cortical  $\gamma$  and  $q$  parameters for several subdivisions of area S1. There was not a significant correlation between the  $\beta$  and  $\gamma$  parameters for area 1 ( $r = 0.26$ ,  $P > 0.10$ ), but there was a significant correlation for the  $p$  and  $q$  parameters ( $r = 0.80$ ,  $P < 0.001$ ). Area 3b demonstrated a significant correlation between the  $\beta$  and  $\gamma$  parameters ( $r = 0.44$ ,  $P < 0.05$ ) and a nearly significant correlation between the  $p$  and  $q$  parameters ( $r = 0.42$ ,  $P = 0.0547$ ). Area 2 (not pictured) did not demonstrate significant correlations neither between the  $\beta$  and  $\gamma$  parameters ( $r = 0.34$ ,  $P = 0.08$ ) nor between the  $p$  and  $q$  parameters ( $r = 0.22$ ,  $P > 0.10$ ). Area 4 ( $r_{\beta \text{ vs. } \gamma} = 0.23$ ;  $r_{p \text{ vs. } q} = 0.09$ ) and area 3a ( $r_{\beta \text{ vs. } \gamma} = 0.28$ ;  $r_{p \text{ vs. } q} = 0.19$ ) also did not have any significant correlations (all  $P > 0.10$ ).

As a second means of determining which areas were most involved in tactile hyperacuity, the number of voxels that were significantly correlated with the stimulus frequency was counted. There was a significant difference in the number of correlated voxels between the 5 areas (1-way ANOVA,  $P < 0.05$ ). Post hoc comparisons indicate that there were more correlated voxels for each of the somatotopic regions compared with area 4, primary motor cortex (Scheffé test, all  $P < 0.05$ ). Although area 2 had far fewer correlated voxels compared with areas 3a, 3b, and 1 (roughly 85%), there was no strong statistical difference ( $P > 0.05$ ). Differences in the number of significant voxels between regions 3a, 3b, and 1 could not be statistically distinguished (Scheffé test, all  $P > 0.10$ ). Figure 3 illustrates that BOLD responses above the 0.27 correlation threshold are localized to the posterior wall of the central sulcus (area 3b) and the crown of the postcentral gyrus (area 1). Fewer responses appear along the floor of the central sulcus (area 3a) or the anterior wall of the postcentral sulcus (area 2). Virtually no responses appear along the anterior wall of the central sulcus (area 4). Thus, areas 3b and 1 appear to account for most of the variability in hyperacuity thresholds because of the larger number of active voxels and because estimates of cortical magnification from these regions are correlated with hyperacuity thresholds across subjects.

Upon visual inspection of the data on the flattened cortical representation, a bimodal distribution of the peak BOLD activity in many subjects was observed (e.g., Fig. 3B). If one assumes that the peak activity is driven by stimulation of the fingertips, then the positioning of the 2 peaks on the flattened cortex reflects

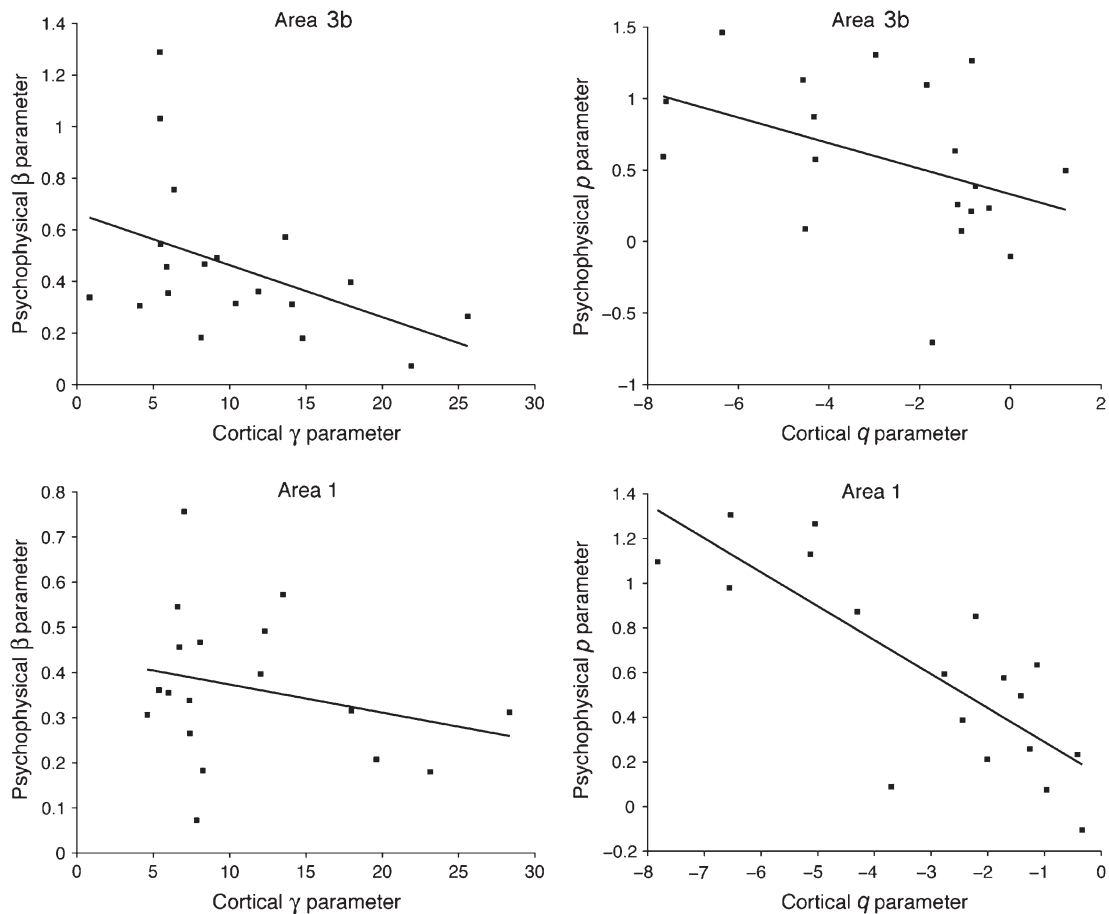


**Figure 7.** Hyperacuity thresholds correlate with cortical magnification for areas 3b and 1. Brodmann areas 1, 2, 3a, 3b, and 4 were estimated using anatomical methods. For each brain area, BOLD activity patterns on the flattened representation were fit with templates, and the cortical magnification for each area was computed. Curve fitting resulted in a set of  $\beta$ ,  $\gamma$ ,  $\rho$ , and  $q$  parameters for each area, which were compared with similar fits to the psychophysical data. There was no significant correlation between the  $\beta$  and  $\gamma$  parameters for area 1 ( $P > 0.10$ ), but there were significant correlations between the  $\rho$  and  $q$  parameters ( $P < 0.001$ ). Area 3b demonstrated a significant correlation for the  $\beta$  and  $\gamma$  parameters ( $P < 0.05$ ) and a borderline significant correlation for the  $\rho$  and  $q$  parameters ( $P = 0.0547$ ). Areas 2, 3a, and 4 (not pictured) did not have any significant correlations (all  $P > 0.08$ ).

the expected mirror-reversal relationship between the representation of the fingers in areas 3b and 1.

### Sources of Error in the Estimation of Cortical Magnification

There are several potential sources of error in the template-fitting technique (see Duncan and Boynton 2003). However, there is one complication that is unique to this study. Suppose the fMRI response for each single finger on the flattened cortex can be described using Gaussian functions that may or may not have an asymmetric aspect ratio. fMRI responses were generated by averaging across 3 scans in which 1 finger was stimulated in alternation with the other 3 fingers. Take as an example the index finger (D2); if the Gaussian functions for D3–D5 were subtracted from the Gaussian function for D2, then the resulting “estimated” fMRI response for D2 will be shifted laterally from its real center, away from the other fingers. The size of this shift is proportional to the width of the underlying Gaussian functions. This effect will be more pronounced for the index finger (D2) and little finger (D5) because they are compared with wholly medial or lateral finger representations, respectively. The main effect of this bias is a general overestimation of cortical magnification (an overestimate of  $\gamma$ ).

There might also be a slight bias to overestimate  $a1$  and  $a3$ , resulting in a small reduction on the slope of the function describing cortical distance for each finger pair.

Spatial blurring is introduced to interpolate the BOLD signal across regions along the flattened cortical surface that do not correspond directly to an active voxel in the 3D manifold. This computational blurring is typically restricted to 1 voxel, which is much less than that associated with physiological hemodynamic blurring. The spatial blurring of the hemodynamic response is known to extend far beyond the neuronal locus of stimulation in visual cortex (Grinvald et al. 1994). However, because the template-fitting method measures the peak-to-peak distance between cortical representations of the fingers, the hemodynamic blurring of the BOLD signal does not adversely affect our estimates of cortical magnification. The blurring of the BOLD signal (e.g., Fig. 3D) is much greater than peak-to-peak distance between finger representations in the cortex (e.g.,  $a3$  from Fig. 3E), especially for fingers D4 and D5. Estimates of the distance between cortical finger representations do not appear to be greatly affected by hemodynamic blurring. Hemodynamic blurring is uniform across finger representations (e.g., Fig. 3A–D) and thus cannot account for the systematic differences

between observers or the correlation with measures of hyperacuity.

### ***Estimating Thresholds and Receptive Field Size from Cortical Magnification***

Hyperacuity is likely to be affected by both the number of neurons representing a given region in space and the spatial profile of their receptive fields. Receptive field size does not necessarily scale directly with cortical magnification. For example, in the primary visual cortex, receptive field size is roughly proportional to areal cortical magnification (ACMF) raised to the negative 2/3 power (Stevens 2002). Receptive field sizes within primate somatosensory cortex also appear to follow this  $-2/3$  power rule (Sur et al. 1980).

Therefore, estimated receptive field size, in square millimeters was estimated from the observed measurements in somatosensory cortex by raising cortical magnification factors to the  $-2/3$  power. To convert receptive field sizes (in units of area, square millimeters) to predicted hyperacuity thresholds (in linear units, millimeter), the square root of the estimated receptive field size was computed (i.e.,  $\tau_{\text{PRED}} = [\text{ACMF}^{-2/3}]^{1/2}$ , where  $\tau_{\text{PRED}}$  equals the predicted threshold). These estimated thresholds are plotted as asterisks in Figure 2. Thresholds agree reasonably well with predictions based on estimates of receptive field size, suggesting that the correlations observed may have been driven by individual differences in receptive field sizes of different fingers.

The thresholds estimated from measurements of cortical magnification (asterisk) were not different than the observed thresholds for 3 of the 4 digits ( $t$ -test, all  $P < 0.0125$ ). However, the estimated threshold for D2 was lower than the observed value ( $P = 0.0042$ ). The estimated and observed thresholds were also compared according to the following procedure. First, a logarithmic transform was applied to the estimated and observed mean thresholds. Second, each data set was fit with a linear regression model. Third, the slopes and intercepts of the fits to each data set were compared using standard methods from simple linear regression (Zar 1999). There was no difference between the 2 data sets for slope or elevation (all  $P > 0.10$ ). Therefore, there is little evidence to suggest that the estimated thresholds differ from the measured thresholds.

Receptive field size can vary greatly with variations in stimulus properties, and fine spatial resolution might be achieved with sharp receptive field profiles. Although the current results suggest a true correlation between tactile hyperacuity and cortical sampling density, further testing using a variety of stimuli should be conducted.

## **Discussion**

### ***Prior Investigations of Tactile Spatial Resolution***

The threshold measurements using the Ludvigh task from this study are slightly higher than those originally obtained by Loomis (1979) and lower than those found using JVP domes (Johnson and Phillips 1981; Van Boven and Johnson 1994; Sathian and Zangaladze 1996; Vega-Bermudez and Johnson 2001). Using a stimulus similar to the one in the present paper, Sathian and Zangaladze (1998) and Grant et al. (2000) found hyperacuity thresholds at the index finger that were close to those in the present paper (mean 0.56 and 0.58 mm, respectively). In the current study, movement of the fingers

was less restricted than in some other studies. The slight temporal asynchrony when a finger came into contact with each of the 3 bumps may have improved discrimination thresholds (Loomis and Collins 1978; Loomis 1979).

Previous studies have reported significantly poorer spatial resolution in D5 than the other 4 fingers using JVP domes (Sathian and Zangaladze 1996), and a significant increase in thresholds across D2–D4 was demonstrated later (Vega-Bermudez and Johnson 2001). The results from the current study were qualitatively similar though the increase in thresholds between D2 and D4 did not reach significance.

The current study differed from 2 previous studies (Sathian and Zangaladze 1996; Vega-Bermudez and Johnson 2001) that did not report a difference in tactile resolution between hands. The hyperacuity task in the current report may tax different physiological mechanisms than the JVP domes and letter recognition tasks used in the previous reports. These differences are made evident by the lower thresholds on the hyperacuity task. The left-handed superiority observed in the current report might be explained by asymmetries in the cortex that are more pronounced for mechanisms encoding hyperacuity. This is not to say that asymmetries could not occur for other tasks. Indeed, the review of Summers and Lederman (1990) demonstrated that, when asymmetries occur, they favor the same side for specific tasks. Interestingly, a larger number of the tasks reviewed demonstrated left-handed superiority (presumably involving the right hemisphere). These tasks included pressure thresholds, 2-point discrimination, discrimination of roughness, and Braille reading. The authors concluded that there was a left-handed bias for tasks that demand spatial mediation and a right-handed bias for tasks that demand verbal mediation. It should also be noted that Sathian and Zangaladze (1996) reported a left-sided asymmetry for one subject. However, because the current report is contingent upon the removal of one outlier and because we did not use multiple stimulus types, strong conclusions should not be based upon these results. The possibility of a type I error must be considered.

### ***Prior Investigations of Cortical Magnification***

Consistent with previous findings, the mean distance between the cortical representations of the index finger and little finger in the current study was 13 mm, and the range across subjects and hemispheres was between 8 and 23 mm (Baumgartner et al. 1991; Sutherling et al. 1992; Kurth et al. 1998; Maldjian et al. 1999; McGlone et al. 2002).

Consistent correlations with hyperacuity thresholds were only found for areas 3b and 1. This result was not surprising considering 1) 3b responds primarily to cutaneous stimulation and 2) the overall representation of 3b varies by more than 2-fold between individuals (Merzenich et al. 1987), which makes 3b a likely substrate to account for individual differences in tactile thresholds. Neurons in area 1 also respond predominantly to cutaneous stimulation, but they have larger receptive fields that limit their ability to resolve fine tactile stimuli (Merzenich et al. 1978; Kaas et al. 1979; Nelson et al. 1980; Sur et al. 1982; Felleman et al. 1983). However, there is not enough evidence to suggest that neither area 3b nor area 1 is uniquely responsible for encoding tactile hyperacuity. The lack of a correlation between hyperacuity thresholds and cortical magnification for areas 3a and 2 is not surprising. A majority of the cells in these areas are driven by deep cutaneous receptors

or joint receptors (Iwamura and Tanaka 1978; Iwamura et al. 1980; Pons et al. 1985; Iwamura et al. 1993; Huffman and Krubitzer 2001).

Similar to the study of Shoham and Grinvald (2001), a gradient in cortical magnification from the index finger to the little finger representation was observed, with the mean distance between representations of D2–D3, D3–D4, and D4–D5 being 6.2, 5.7, and 1.1 mm, respectively.

One fMRI study found a correlation between the change in psychophysical thresholds and the change in the size of the index finger representation after tactile coactivation of adjacent regions on the surface of the skin (Pleger et al. 2003). However, because they used a relative metric, the study of Pleger et al. could not look at the baseline correlation between thresholds and cortical magnification. Furthermore, the study only looked at 1 finger, which limits the generalization of their findings. This study is the first to determine the correlation between tactile hyperacuity and cortical magnification across fingers, implicating areas 3b and 1 within S1 as loci for critical factors in hyperacuity.

The intersubject variations in this study and the study of Merzenich et al. (1987) contradict previous histology studies in nonhuman primates that did not find variation between the cortical representation of the digits (Jain et al. 1998; Qi and Kaas 2004). One possible explanation for this apparent contradiction is that functional representations measured with fMRI may vary more than anatomical representations measured with histology. Species-specific differences may also explain this discrepancy.

### ***The Relationship between Cortical Magnification and Receptor Density***

It has often been assumed that variations in spatial resolution can be attributed to Merkel disks, which are mechanoreceptors with small receptive fields and SA1 afferents that densely populate the dermis of the fingers (Vallbo and Johansson 1978; Johansson and Vallbo 1979; Darian-Smith and Kenis 1980). Histologically identified Merkel disks correspond to physiologically identified SA1 afferents. Importantly, changes in their density alone may not explain the increase in thresholds from the index finger to the little finger because they appear to be uniformly distributed across the fingertips (Vallbo and Johansson 1978; Pare et al. 2002). Furthermore, there are several examples where the periphery is represented more extensively than indicated by receptor density. For example, the fovea in monkey V1 has a disproportionately larger representation than the peripheral retina (Azzopardi and Cowey 1993). Additionally, cortical magnification varies across the touch organs of the star-faced mole (Catania 1995; Catania and Kaas 1997).

Instead, the difference in thresholds between fingers may result from a sampling bias downstream from the spinal cord. The little finger, for example, has a smaller representation than the other fingers in the dorsal column nuclei in the cuneate nucleus (CN) of the medulla (Xu and Wall 1999). Also, the divergence from the central cutaneous core of ventral posterior lateral thalamus (VPL) to area 3b of primary somatosensory cortex (S1) is extensive; 25 mm<sup>2</sup> of cortex is subtended by 0.1 mm<sup>3</sup> of VPL (Rausell et al. 1998). This extensive divergence and convergence between the thalamus and cortex may better account for variations in thresholds than variations in mechanoreceptor density alone. Nevertheless, despite the results

of the current study and the results from one histological experiment that found a lack of variation in innervation of the digits (Pare et al. 2002), innervation density may still contribute to variations in spatial acuity, even if only in part.

The current study cannot conclusively localize the source of variability on the hyperacuity task to S1. To do so would require comparing finger representations at the brain stem, thalamus, and cortex. To our knowledge, no such study has been completed. In their elegant histological study, Rausell et al. (1998) determined that there was extensive convergence and divergence between the thalamus and the cortex. Additionally, there is evidence of exaggerated representations of the hand as early as the CN of the medulla (Xu and Wall 1999), which suggests that cortical magnification is a gradual process that accelerates with increased distance from the periphery. This notion is further supported by the observation that innervation density at the periphery does not vary greatly between digits (Pare et al. 2002). Taken in isolation, none of these studies prove that S1 is the physiological correlate for hyperacuity. The current report is important because it provides the first evidence that cortical magnification accounts for much of the interdigit variability on a hyperacuity task in humans.

### ***The Role of Plasticity in Primary Sensory Cortex***

It might be considered somewhat counterintuitive for primary sensory cortex to be a major “bottleneck” for sensory acuity; after all, why sample a sensory domain with finer detail than necessary? One possibility is that it is more efficient to oversample a sensory domain at the receptor or the thalamic level than in the greatly expanded representation of sensory cortex and that in the case of training or deprivation (such as the loss of a limb or a visual scotoma) the cortex can make good use of the “excess sampling capacity.” Interestingly, the effects of deprivation or training in adult visual cortex seem to be fairly limited, suggesting that the correlation between visual acuity and cortical size found in our previous study may be primarily established in development.

Visual hyperacuity, but not visual acuity, was shown to improve with practice (Westheimer 2001). Similarly, psychophysical evidence demonstrates an improvement in hyperacuity thresholds with training (Sathian and Zangaladze 1998; Grant et al. 2000). Superior tactile hyperacuity (Grant et al. 2000) and acuity of the blind has also been demonstrated (reviewed in Sathian 2000). Effects of training and deprivation on both receptive field size and the cortical area devoted to each finger have also been demonstrated within adult monkey somatosensory cortex (Recanzone et al. 1992; Xerri et al. 1999). Also, musicians with dystonia undergo cortical reorganization after therapy (Candia et al. 2003), and manipulations of attention also affect somatotopic representations in S1 (Johansen-Berg et al. 2000; Braun et al. 2002; Hamalainen et al. 2002; Meador et al. 2002). Finally, an fMRI study in humans has found a correlation between the change in psychophysical thresholds and the change in the size of the index finger representation after tactile coactivation of adjacent regions on the surface of the skin (Pleger et al. 2003). The adult somatosensory cortex is clearly capable of both short- and long-term plasticity.

Descending projections from S1 to thalamus outnumber ascending projection by as many as 10 to 1 (Liu et al. 1995). This wiring scheme appears ideal for “top-down” shaping of receptive fields. For example, injecting an N-methyl-D-aspartic

acid antagonist directly into area 3b dramatically alters the receptive fields of the fingers, and in some cases the receptive fields grow to encompass multiple fingers (Ergenzinger et al. 1998). Cortex has a role in shaping how tactile information is processed at earlier stages, and a greater understanding of the relationship between tactile thresholds and somatotopic organization may shed light upon the issue of plasticity.

### Summary

To our knowledge, no previous study has provided either a direct or indirect comparison between hyperacuity and cortical magnification for different fingers in the same human subjects. The slope of the changes in cortical magnification across cortical finger representations in S1 was significantly correlated with changes in thresholds from the index finger to the little finger. This result implicates S1 as a possible limiting site for tactile hyperacuity.

In a previous study, we have demonstrated that acuity across the visual field was similarly correlated with cortical magnification within V1 (Duncan and Boynton 2003). It seems that these results may speak to a general property of primary sensory cortex as a bottleneck for sensory acuity.

### Notes

The authors would like to thank A. Cyrus Arman for technical assistance and Vivian Ciaramitaro, Ione Fine, Sara Mednick, Minna Ng, and August Tuan for helpful comments on drafts of the manuscript. This study was supported by National Institute of Health grants EY07028-02 and EY12925. *Conflict of Interest:* None declared.

Funding to pay the Open Access publication charges for this article was provided by National Institute of Health grants EY07028-02 and EY12925.

Address correspondence to Dr Robert O. Duncan, PhD, Hamilton Glaucoma Center, University of California, San Diego, 9500 Gilman Drive, La Jolla, CA 92093-0946, USA. Email: rduncan@eyecenter.ucsd.edu.

### References

Allison T, McCarthy G, Wood CC, Williamson PD, Spencer DD. 1989. Human cortical potentials evoked by stimulation of the median nerve. II. Cytoarchitectonic areas generating long-latency activity. *J Neurophysiol.* 62:711-722.

Arun KS, Huang TS, Blotstein SD. 1987. Least-squares fitting of two 3-d point sets. *IEEE PAMI.* 9:698-700.

Azzopardi P, Cowey A. 1993. Preferential representation of the fovea in the primary visual cortex. *Nature.* 361:719-721.

Baumgartner C, Doppelbauer A, Deecke L, Barth DS, Zeitlhofer J, Lindinger G, Sutherling WW. 1991. Neuromagnetic investigation of somatotopy of human hand somatosensory cortex. *Exp Brain Res.* 87:641-648.

Blankenburg F, Ruben J, Meyer R, Schwimann J, Villringer A. 2003. Evidence for a rostral-to-caudal somatotopic organization in human primary somatosensory cortex with mirror-reversal in areas 3b and 1. *Cereb Cortex.* 13:987-993.

Boynton GM, Demb JB, Glover GH, Heeger DJ. 1999. Neuronal basis of contrast discrimination. *Vision Res.* 39:257-269.

Boynton GM, Engel SA, Glover GH, Heeger DJ. 1996. Linear systems analysis of functional magnetic resonance imaging in human V1. *J Neurosci.* 16:4207-4221.

Brainard DH. 1997. The Psychophysics Toolbox. *Spat Vision.* 10:433-436.

Braun C, Haug M, Wiech K, Birbaumer N, Elbert T, Roberts LE. 2002. Functional organization of primary somatosensory cortex depends on the focus of attention. *Neuroimage.* 17:1451-1458.

Braun C, Schweizer R, Elbert T, Birbaumer N, Taub E. 2000. Differential activation in somatosensory cortex for different discrimination tasks. *J Neurosci.* 20:446-450.

Brodmann K. 1909. Vergleichende lokalisation der grosshirnrinde in ihren prinzipien dargestellt auf grund des zellenbaues. Leipzig, (Germany): Barth.

Buchner H, Reinartz U, Waberski TD, Gobbele R, Noppeney U, Scherg M. 1999. Sustained attention modulates the immediate effect of deafferentation on the cortical representation of the digits: source localization of somatosensory evoked potentials in humans. *Neurosci Lett.* 260:57-60.

Buchner H, Richrath P, Grunholz J, Noppeney U, Waberski TD, Gobbele R, Willmes K, Treede RD. 2000. Differential effects of pain and spatial attention on digit representation in the human primary somatosensory cortex. *Neuroreport.* 11:1289-1293.

Candia V, Wienbruch C, Elbert T, Rockstroh B, Ray W. 2003. Effective behavioral treatment of focal hand dystonia in musicians alters somatosensory cortical organization. *Proc Natl Acad Sci USA.* 100:7942-7946.

Catania KC, Kaas JH. 1997. Somatosensory fovea in the star-nosed mole: behavioral use of the star in relation to innervation patterns and cortical representation. *J Comp Neurol.* 387:215-233.

Catania KG. 1995. Magnified cortex in star-nosed moles. *Nature.* 375:453-454.

Darian-Smith I, Kenins P. 1980. Innervation density of mechanoreceptive fibres supplying glabrous skin of the monkey's index finger. *J Physiol.* 309:147-155.

Dechent P, Frahm J. 2003. Functional somatotopy of finger representations in human primary motor cortex. *Hum Brain Mapp.* 18:272-283.

Duncan RO, Boynton GM. 2003. Cortical magnification within human primary visual cortex correlates with acuity thresholds. *Neuron.* 38:659-671.

Elbert T, Pantev C, Wienbruch C, Rockstroh B, Taub E. 1995. Increased cortical representation of the fingers of the left hand in string players. *Science.* 270:305-307.

Engel SA, Glover GH, Wandell BA. 1997. Retinotopic organization in human visual cortex and the spatial precision of functional MRI. *Cereb Cortex.* 7:181-192.

Engel SA, Rumelhart DE, Wandell BA, Lee AT, Glover GH, Chichilnisky EJ, Shadlen MN. 1994. fMRI of human visual cortex. *Nature.* 369:525.

Ergenzinger ER, Glasier MM, Hahn JO, Pons TP. 1998. Cortically induced thalamic plasticity in the primate somatosensory system. *Nat Neurosci.* 1:226-229.

Felleman DJ, Nelson RJ, Sur M, Kaas JH. 1983. Representations of the body surface in areas 3b and 1 of postcentral parietal cortex of Cebus monkeys. *Brain Res.* 268:15-26.

Francis ST, Kelly EF, Bowtell R, Dunseath WJ, Folger SE, McGlone F. 2000. fMRI of the responses to vibratory stimulation of digit tips. *Neuroimage.* 11:188-202.

Gelnar PA, Krauss BR, Szeverenyi NM, Apkarian AV. 1998. Fingertip representation in the human somatosensory cortex: an fMRI study. *Neuroimage.* 7:261-283.

Geyer S, Schleicher A, Zilles K. 1997. The somatosensory cortex of human: cytoarchitecture and regional distributions of receptor-binding sites. *Neuroimage.* 6:27-45.

Geyer S, Schleicher A, Zilles K. 1999. Areas 3a, 3b, and 1 of human primary somatosensory cortex. *Neuroimage.* 10:63-83.

Grant AC, Thiagarajah MC, Sathian K. 2000. Tactile perception in blind Braille readers: a psychophysical study of acuity and hyperacuity using gratings and dot patterns. *Percept Psychophys.* 62:301-312.

Grinvald A, Lieke EE, Frostig RD, Hildesheim R. 1994. Cortical point-spread function and long-range lateral interactions revealed by real-time optical imaging of macaque monkey primary visual cortex. *J Neurosci.* 14:2545-2568.

Hamalainen H, Hiltunen J, Titievskaja I. 2002. Activation of somatosensory cortical areas varies with attentional state: an fMRI study. *Behav Brain Res.* 135:159-165.

Huffman KJ, Krubitzer L. 2001. Area 3a: topographic organization and cortical connections in marmoset monkeys. *Cereb Cortex.* 11:849-867.

- Iwamura Y, Tanaka M. 1978. Postcentral neurons in hand region of area 2: their possible role in the form discrimination of tactile objects. *Brain Res.* 150:662-666.
- Iwamura Y, Tanaka M, Hikosaka O. 1980. Overlapping representation of fingers in the somatosensory cortex (area 2) of the conscious monkey. *Brain Res.* 197:516-520.
- Iwamura Y, Tanaka M, Sakamoto M, Hikosaka O. 1993. Rostrocaudal gradients in the neuronal receptive field complexity in the finger region of the alert monkey's postcentral gyrus. *Exp Brain Res.* 92:360-368.
- Jain N, Catania KC, Kaas JH. 1998. A histologically visible representation of the fingers and palm in primate area 3b and its immutability following long-term deafferentations. *Cereb Cortex.* 8:227-236.
- Johansen-Berg H, Christensen V, Woolrich M, Matthews PM. 2000. Attention to touch modulates activity in both primary and secondary somatosensory areas. *Neuroreport.* 11:1237-1241.
- Johansson RS, Vallbo AB. 1979. Tactile sensibility in the human hand: relative and absolute densities of four types of mechanoreceptive units in glabrous skin. *J Physiol.* 286:283-300.
- Johnson KO, Phillips JR. 1981. Tactile spatial resolution. I. Two-point discrimination, gap detection, grating resolution, and letter recognition. *J Neurophysiol.* 46:1177-1192.
- Kaas JH. 1983. What, if anything, is SI? Organization of first somatosensory area of cortex. *Physiol Rev.* 63:206-231.
- Kaas JH, Nelson RJ, Sur M, Lin CS, Merzenich MM. 1979. Multiple representations of the body within the primary somatosensory cortex of primates. *Science.* 204:521-523.
- Kennett S, Taylor-Clarke M, Haggard P. 2001. Noninformative vision improves the spatial resolution of touch in humans. *Curr Biol.* 11:1188-1191.
- Kurth R, Villringer K, Mackert BM, Schwiemann J, Braun J, Curio G, Villringer A, Wolf KJ. 1998. fMRI assessment of somatotopy in human Brodmann area 3b by electrical finger stimulation. *Neuroreport.* 9:207-212.
- Liu XB, Honda CN, Jones EG. 1995. Distribution of four types of synapse on physiologically identified relay neurons in the ventral posterior thalamic nucleus of the cat. *J Comp Neurol.* 352:69-91.
- Loomis JM. 1979. An investigation of tactile hyperacuity. *Sens Processes.* 3:289-302.
- Loomis JM, Collins CC. 1978. Sensitivity to shifts of a point stimulus: an instance of tactile hyperacuity. *Percept Psychophys.* 24:487-492.
- Ludvig E. 1953. Direction sense of the eye. *Am J Ophthalmol.* 36:139-143.
- Maldjian JA, Gottschalk A, Patel RS, Detre JA, Alsop DC. 1999. The sensory somatotopic map of the human hand demonstrated at 4 Tesla. *Neuroimage.* 10:55-62.
- McGlone F, Kelly EF, Trullsson M, Francis ST, Westling G, Bowtell R. 2002. Functional neuroimaging studies of human somatosensory cortex. *Behav Brain Res.* 135:147-158.
- Meador KJ, Allison JD, Loring DW, Lavin TB, Pillai JJ. 2002. Topography of somatosensory processing: cerebral lateralization and focused attention. *J Int Neuropsychol Soc.* 8:349-359.
- Meador KJ, Ray PG, Day L, Ghelani H, Loring DW. 1998. Physiology of somatosensory perception: cerebral lateralization and extinction. *Neurology.* 51:721-727.
- Merzenich MM, Kaas JH, Sur M, Lin CS. 1978. Double representation of the body surface within cytoarchitectonic areas 3b and 1 in "SI" in the owl monkey (*Aotus trivirgatus*). *J Comp Neurol.* 181:41-73.
- Merzenich MM, Nelson RJ, Kaas JH, Stryker MP, Jenkins WM, Zook JM, Cynader MS, Schoppmann A. 1987. Variability in hand surface representations in areas 3b and 1 in adult owl and squirrel monkeys. *J Comp Neurol.* 258:281-296.
- Moore CI, Stern CE, Corkin S, Fischl B, Gray AC, Rosen BR, Dale AM. 2000. Segregation of somatosensory activation in the human Rolandic cortex using fMRI. *J Neurophysiol.* 84:558-569.
- Nelson RJ, Sur M, Felleman DJ, Kaas JH. 1980. Representations of the body surface in postcentral parietal cortex of *Macaca fascicularis*. *J Comp Neurol.* 192:611-643.
- Noppeney U, Waberski TD, Gobbels R, Buchner H. 1999. Spatial attention modulates the cortical somatosensory representation of the digits in humans. *Neuroreport.* 10:3137-3141.
- Ono M, Kubik S, Abernathy CD. 1990. Atlas of the cerebral sulci. Stuttgart (Germany): Thieme.
- Overduin SA, Servos P. 2004. Distributed digit somatotopy in primary somatosensory cortex. *Neuroimage.* 23:462-472.
- Pantev C, Engelien A, Candia V, Elbert T. 2001. Representational cortex in musicians. Plastic alterations in response to musical practice. *Ann NY Acad Sci.* 930:300-314.
- Pare M, Smith AM, Rice FL. 2002. Distribution and terminal arborizations of cutaneous mechanoreceptors in the glabrous finger pads of the monkey. *J Comp Neurol.* 445:347-359.
- Pascual-Leone A, Torres F. 1993. Plasticity of the sensorimotor cortex representation of the reading finger in Braille readers. *Brain.* 116(Pt 1):39-52.
- Pelli DG. 1997. The VideoToolbox software for visual psychophysics: transforming numbers into movies. *Spat Vis.* 10:437-442.
- Pleger B, Foerster AF, Ragert P, Dinse HR, Schwenkreis P, Malin JP, Nicolas V, Tegenthoff M. 2003. Functional imaging of perceptual learning in human primary and secondary somatosensory cortex. *Neuron.* 40:643-653.
- Pons TP, Garraghty PE, Cusick CG, Kaas JH. 1985. The somatotopic organization of area 2 in macaque monkeys. *J Comp Neurol.* 241:445-466.
- Powell TP, Mountcastle VB. 1959. The cytoarchitecture of the postcentral gyrus of the monkey *Macaca mulatta*. *Bull Johns Hopkins Hosp.* 105:108-131.
- Qi HX, Kaas JH. 2004. Myelin stains reveal an anatomical framework for the representation of the digits in somatosensory area 3b of macaque monkeys. *J Comp Neurol.* 477:172-187.
- Rademacher J, Buegel U, Geyer S, Schormann T, Schleicher A, Freund HJ, Zilles K. 2001. Variability and asymmetry in the human precentral motor system. A cytoarchitectonic and myeloarchitectonic brain mapping study. *Brain.* 124:2232-2258.
- Rausell E, Bickford L, Manger PR, Woods TM, Jones EG. 1998. Extensive divergence and convergence in the thalamocortical projection to monkey somatosensory cortex. *J Neurosci.* 18:4216-4232.
- Recanzone GH, Merzenich MM, Jenkins WM, Grajski KA, Dinse HR. 1992. Topographic reorganization of the hand representation in cortical area 3b owl monkeys trained in a frequency-discrimination task. *J Neurophysiol.* 67:1031-1056.
- Rumeau C, Tzourio N, Murayama N, Peretti-Viton P, Levrier O, Joliot M, Mazoyer B, Salamon G. 1994. Location of hand function in the sensorimotor cortex: MR and functional correlation. *AJNR (Am J Neuroradiol.)* 15:567-572.
- Sathian K. 2000. Practice makes perfect: sharper tactile perception in the blind. *Neurology.* 54:2203-2204.
- Sathian K, Zangaladze A. 1996. Tactile spatial acuity at the human fingertip and lip: bilateral symmetry and interdigit variability. *Neurology.* 46:1464-1466.
- Sathian K, Zangaladze A. 1998. Perceptual learning in tactile hyperacuity: complete intermanual transfer but limited retention. *Exp Brain Res.* 118:131-134.
- Sereno MI, Dale AM, Reppas JB, Kwong KK, Belliveau JW, Brady TJ, Rosen BR, Tootell RB. 1995. Borders of multiple visual areas in humans revealed by functional magnetic resonance imaging. *Science.* 268:889-893.
- Shoham D, Grinvald A. 2001. The cortical representation of the hand in macaque and human area S-I: high resolution optical imaging. *J Neurosci.* 21:6820-6835.
- Smith AT, Williams AL, Singh KD. 2004. Negative BOLD in the visual cortex: evidence against blood stealing. *Hum Brain Mapp.* 21:213-220.
- Sobel DF, Gallen CC, Schwartz BJ, Waltz TA, Copeland B, Yamada S, Hirschkoff EC, Bloom FE. 1993. Locating the central sulcus: comparison of MR anatomic and magnetoencephalographic functional methods. *AJNR Am J Neuroradiol.* 14:915-925.
- Stevens CF. 2001. An evolutionary scaling law for the primate visual system and its basis in cortical function. *Nature.* 411:193-195.
- Stevens CF. 2002. Predicting functional properties of visual cortex from an evolutionary scaling law. *Neuron.* 36:139-142.

- Stevens JC, Patterson MQ. 1995. Dimensions of spatial acuity in the touch sense: changes over the life span. *Somatosens Mot Res.* 12:29-47.
- Summers DC, Lederman SJ. 1990. Perceptual asymmetries in the somatosensory system: a dichhaptic experiment and critical review of the literature from 1929 to 1986. *Cortex.* 26:201-226.
- Sur M, Merzenich MM, Kaas JH. 1980. Magnification, receptive-field area, and "hypercolumn" size in areas 3b and 1 of somatosensory cortex in owl monkeys. *J Neurophysiol.* 44:295-311.
- Sur M, Nelson RJ, Kaas JH. 1982. Representations of the body surface in cortical areas 3b and 1 of squirrel monkeys: comparisons with other primates. *J Comp Neurol.* 211:177-192.
- Sutherland WW, Levesque MF, Baumgartner C. 1992. Cortical sensory representation of the human hand: size of finger regions and nonoverlapping digit somatotopy. *Neurology.* 42:1020-1028.
- Teo PC, Sapiro G, Wandell BA. 1997. Creating connected representations of cortical gray matter for functional MRI visualization. *IEEE Trans Med Imaging.* 16:852-863.
- Towle VL, Khorasani L, Uftring S, Pelizzari C, Erickson RK, Spire JP, Hoffmann K, Chu D, Scherg M. 2003. Noninvasive identification of human central sulcus: a comparison of gyral morphology, functional MRI, dipole localization, and direct cortical mapping. *Neuroimage.* 19:684-697.
- Vallbo AB, Johansson RS. 1978. The tactile sensory innervation of the glabrous skin of the human hand. In: Gordon G, editors. *Active touch: the mechanism of recognition of objects by manipulation. A multidisciplinary approach.* Oxford: Pergamon Press. p. 29-54.
- Van Boven RW, Johnson KO. 1994. A psychophysical study of the mechanisms of sensory recovery following nerve injury in humans. *Brain.* 117(Pt 1):149-167.
- Vega-Bermudez F, Johnson KO. 2001. Differences in spatial acuity between digits. *Neurology.* 56:1389-1391.
- Vogt C, Vogt O. 1919. Allgemeinere Ergebnisse unserer Hirnforschung. *J Psychol Neurophysiol.* 25:279-462.
- Westheimer G. 1977. Spatial frequency and light-spread descriptions of visual acuity and hyperacuity. *J Opt Soc Am.* 67:207-212.
- Westheimer G. 2001. Is peripheral visual acuity susceptible to perceptual learning in the adult? *Vision Res.* 41:47-52.
- Wheat HE, Goodwin AW, Browning AS. 1995. Tactile resolution: peripheral neural mechanisms underlying the human capacity to determine positions of objects contacting the fingerpad. *J Neurosci.* 15:5582-5595.
- White LE, Andrews TJ, Hulette C, Richards A, Groelle M, Paydarfar J, Purves D. 1997. Structure of the human sensorimotor system. I: morphology and cytoarchitecture of the central sulcus. *Cereb Cortex.* 7:18-30.
- Xerri C, Merzenich MM, Jenkins W, Santucci S. 1999. Representational plasticity in cortical area 3b paralleling tactual-motor skill acquisition in adult monkeys. *Cereb Cortex.* 9:264-276.
- Xu J, Wall JT. 1999. Functional organization of tactile inputs from the hand in the cuneate nucleus and its relationship to organization in the somatosensory cortex. *J Comp Neurol.* 411:369-389.
- Yousry TA, Schmid UD, Alkadhi H, Schmidt D, Peraud A, Buettnner A, Winkler P. 1997. Localization of the motor hand area to a knob on the precentral gyrus. A new landmark. *Brain.* 120(Pt 1):141-157.
- Zar JH. 1999. *Biostatistical analysis.* 4th ed. New Jersey: Prentice Hall.
- Ziemus B, Huonker R, Haueisen J, Liepert J, Spengler F, Weiller C. 2000. Effects of passive tactile co-activation on median ulnar nerve representation in human SI. *Neuroreport.* 11:1285-1288.
- Zilles K, Schlaug G, Matelli M, Luppino G, Schleicher A, Qu M, Dabringhaus A, Seitz R, Roland PE. 1995. Mapping of human and macaque sensorimotor areas by integrating architectonic, transmitter receptor, MRI and PET data. *J Anat.* 187(Pt 3): 515-537.